RSC Advances

PAPER

View Article Online
View Journal | View Issue

Cite this: *RSC Adv.*, 2019, **9**, 34184

Bioassay-guided purification of sesquiterpenoids from the fruiting bodies of *Fomitopsis pinicola* and their anti-inflammatory activity†

Shih-Huang Tai,‡[a] Ping-Chung Kuo,‡[b] Ching-Che Hung,[c] Ying-Hsuan Lin,[d] Tsong-Long Hwang,[e] Sio Hong Lam,[b] Daih-Huang Kuo,[f] Jin-Bin Wu,[g] Hsin-Yi Hung*[b] and Tian-Shung Wu*[bf]

Received 30th July 2019
Accepted 12th September 2019

DOI: 10.1039/c9ra05899k

rsc.li/rsc-advances

Twelve undescribed sesquiterpenoids, fomitopins A–L (**1–12**), were isolated *via* bioassay-guided purification from the bracket fungus *Fomitopsis pinicola* (Sw.) P. Karst, and this fungus have been reported to exhibit anti-microbial and anti-inflammatory activities. The structures of **1–12** were elucidated by spectroscopic and spectrometric analyses and their absolute configurations were further confirmed by ECD simulations. Ten isolated compounds were evaluated for their anti-inflammatory potential and compound **11** exhibited the most significant inhibition of superoxide anion generation and elastase release with IC_{50} values of 0.81 ± 0.15 and 0.74 ± 0.12 μM. These newly purified sesquiterpenoids could be potential candidates for further anti-inflammatory studies.

Introduction

The dried fruiting bodies of different *Fomitopsis* species have been used in folk medicine and have been reported to be associated with antitumor,[1] antibacterial,[2] and immunotropic[3] effects. Among these species, *F. pinicola* (Sw.) P. Karst (Fomitopsidaceae), a red banded polypore found on decaying logs including *Abies*, and *Betula*, throughout temperate regions, is widely distributed in East Asia and Central Europe.[4] A close species, *Fomitopsis marginata* (previous *Polyporous marginata*), looks lighter in color and ungulate, while *Fomitopsis pinicola* is more black and cinnamon.[4] Traditionally, *F. pinicola* is cooked and the decoction used for the treatment of headaches, nausea, liver problems, hemorrhage and inflammation.[5] Pharmacological studies revealed the chloroform extract of *F. pinicola* possesses antitumor activities against hepatoma, lung cancer, colorectal cancer and breast cancer.[6] Moreover, alkali extracts rich in polysaccharides exhibited anti-hyperglycemic effects.[7,8] In addition, lanostanoid derivatives as well as triterpenes were isolated and the isolated steroids showed antimicrobial activity against *Bacillus subtilis* in a TLC bioassay.[9]

Inflammation is known to play key roles in many disease conditions, such as Alzheimer's disease, diabetes, infection, psoriasis, wound, colitis, arthritis, atherosclerosis, immune-diseases and cancers.[10] Addition of the inflammatory disease costs resulted in more than billion dollars in Global drug markets. In 2005, twelve glycosidic triterpenes isolated from *F. pinicola* by Yoshikawa *et al.* exhibited anti-inflammatory activity *via* cyclooxygenase-2 inhibition. The most potent compound, fomitoside E, showed IC_{50} value of 0.15 μM, while clinical used NSAID indomethacin had IC_{50} of 0.6 μM.[11] Moreover, ethanol extract of *F. pinicola* can suppress interferon-γ-induced inflammation marker, IP-10 in a dose-dependent manner.[12] Therefore, in continuity of seeking anti-inflammatory agents for new drug development in our program, this study aimed at isolation of anti-inflammatory principals of *F. pinicola* using bioassay-guided fractionation. Superoxide anion generation and elastase release from human neutrophil were measured as inflammation markers. Normally, under acute inflammation, reactive oxygen species (ROS) and lysosomal enzymes (ex. elastase) will be released to kill microorganism. Once neutrophils

[a]*Departments of Surgery and Anesthesiology, Institute of Biomedical Engineering, National Cheng Kung University, Medical Center and Medical School, Tainan 701, Taiwan*

[b]*School of Pharmacy, College of Medicine, National Cheng Kung University, Tainan 70101, Taiwan. E-mail: tswu@mail.ncku.edu.tw; z10308005@email.ncku.edu.tw; Fax: +886-6-2740552; +886-6-2373149; Tel: +886-6-2747538; +886-6-2353535 ext. 6803*

[c]*Department of Chemistry, National Cheng Kung University, Tainan 70101, Taiwan*

[d]*Department of Environmental Sciences, University of California, Riverside, California 92521, USA*

[e]*Graduate Institute of Natural Products, College of Medicine, Chang Gung University, Research Center for Industry of Human Ecology, Research Center for Chinese Herbal Medicine, Graduate Institute of Health Industry Technology, College of Human Ecology, Chang Gung University of Science and Technology, Department of Anesthesiology, Chang Gung Memorial Hospital, Taoyuan 333, Taiwan*

[f]*Department of Pharmacy, College of Pharmacy and Health Care, Tajen University, Pingtung 907, Taiwan*

[g]*Jen-Li Biotechnology Company, Taichung, Taiwan*

† Electronic supplementary information (ESI) available. CCDC 1573301. For ESI and crystallographic data in CIF or other electronic format see DOI: 10.1039/c9ra05899k

‡ The authors contribute equally to this work.

persist beyond acute inflammation, chronic inflammation initiate and perpetuate, leading to various diseases.[13] Currently, the known chemical constituents from *F. pinicola* mostly belong to steroids and triterpenoids.[5] Minors are terpenoids, sesquiterpenoids and coumarins.[5] Other related polypore species, such as *Laetiporus sulphureus*, *Fomes fomentarius*, *Piptoporus betulinus* and *Laricifomes officinalis*, are also found to rich in triterpenoids and organic acids. Organic solvent extracts from these five species have been evaluated for anti-oxidant, antimicrobial and cytotoxic effects.[5] After screening the ethanol extract of *F. pinicola* as well as six fractions for anti-inflammatory activities, we focused on the purification of fractions 4 to 6 with significant bioactivities. Twelve undescribed sesquiterpenes were found and their structures were elucidated by ^{1}H-, ^{13}C-, 2D-NMR, MS, and ECD spectroscopic and spectrometric analyses. Among these twelve compounds, ten compounds with enough quantity were subjected to further evaluation for anti-inflammatory activities.

Results and discussion

The fruiting bodies of *F. pinicola* were refluxed with EtOH and the extract was concentrated under reduced pressure to give a dark-brown syrup. The EtOH crude extract was subjected to Diaion HP-20 gel column chromatography to afford six major fractions (FPs 1–6), being submitted for superoxide anion generation and elastase release inhibition assays. The results (Table S103†) showed that FP5 (10 μg) had the best inhibition ability of superoxide anion and FPs 4–6 (10 μg) displayed significant inhibition of elastase release (94, 95, 89%, respectively). Therefore, further isolation was performed mainly on fractions 4–6 (FPs 4–6) and these fractions afforded twelve undescribed sesquiterpenes (**1–12**). The structures of these compounds were elucidated as described below.

Fomitopin A (**1**) was obtained as colorless needles with a pseudo-molecular formula of $C_{15}H_{18}O_4Na$ by HRESIMS (*m*/*z* 285.1097 $[M + Na]^+$, calcd for 285.1097), representing seven unsaturation equivalents. The UV (λ_{max} 287, 242 and 216 nm) and IR spectrum (ν_{max} 3420, 3243, 1741 and 1423 cm^{-1}) indicated the absorption of a hydroxyl group, a lactone group and an aromatic unit. The ^{1}H NMR spectrum of **1** (Table 1) showed signals for two aromatic protons at δ_H 6.74 (1H, s, H-9) and 6.64 (1H, s, H-12), an oxymethylene at δ_H 4.85 (2H, s, H-15), and two methyl groups at δ_H 0.93 (3H, s, CH_3-13) and 1.10 (3H, s, CH_3-14), respectively. The ^{13}C and DEPT-135 combined with HSQC NMR spectrum of **1** revealed 15 signals, of which were one carbonyl at δ 173.6, four aromatic quaternary carbons (δ 122.9, 134.4, 144.7, 152.9), two aromatic tertiary carbons (δ 115.1, 113.0), two quaternary carbons (δ 47.1, 50.7), four methylene carbons (δ 19.7, 29.0, 29.6, 64.4) and two methyl carbons (δ 19.8, 25.1). Analysis of HMBC spectrum (Fig. 3) revealed correlations of Me-13 (δ 0.93) and Me-14 (δ 1.10) to C-3 (δ 29.0), C-5 (δ 29.6), C-2 (δ 50.7) and C-6 (δ 47.1). Me-13 also showed correlation with C-1 (δ 173.6), while Me-14 correlated with C-7 (δ 134.4). Moreover, ^{2}J, ^{3}J-HMBC correlations from H-15 (δ 4.85) to C-9 (δ 115.1), C-10 (δ 122.9) and C-11 (δ 152.9); from H-9 (δ 6.7) to C-7 (δ 134.4), C-8 (δ 144.7), C-11 (δ 152.9) and C-15 (δ 64.4); and from H-12 (δ 6.64) to C-6 (δ 47.1), C-8 (δ 144.7), C-10 (δ 122.9) and C-11 (δ 152.9) constructed the basic skeleton of **1**. ^{1}H–^{1}H COSY spectrum of **1** also revealed mutual correlations among H-3 (δ 2.17, 1.76), H-4 (δ 1.97) and H-5 (δ 1.98, 1.86). The relative configuration was determined by X-ray single-crystal diffraction using Cu Kα radiation and the result assigned C-2 and C-6 as *S* and *R* configurations, respectively (Fig. 4). These results were further supported by optical rotatory power ($[\alpha]_D^{25}$ −109.0). The negative value is the same as that of (−)-herbertenolide,[14] while (3*aR*,9*bS*)-3*a*,8,9*b*-trimethyl-1,3,3*a*,9*b*-tetrahydrocyclopenta[*c*]chromen-4(2*H*)-one with opposite ring junction has positive value.[15] Moreover, the proton spectrum also established the *trans* relationship between two vicinal methyl group. In order to confirm the absolute configuration of the ring junction, we performed simulation of ECD spectra *via* Gaussian 09 (Fig. 1). The simulated ECD spectrum showed the same trend as the experimental spectrum that a negative Cotton effect was observed at 249 nm and a positive Cotton effect was observed at 226 nm, which strongly supported 2*S*, 6*R* configurations. Therefore, the structure of compound **1** was assigned as shown based on above elucidations (Fig. 2). Although the structure of **1** is simple, there are not many similar sesquiterpenes discovered in nature. The most similar compound is (−)-herbertenolide[14] with the same lactone herbertenoid structure, but different substitution on phenyl rings.

The UV and IR absorption characteristics of **2–12** were all similar to those of **1**. Fomitopin B (**2**) was obtained as colorless solid and its molecular formula was determined as $C_{17}H_{22}O_4$ by HRESIMS analysis. The ^{1}H and ^{13}C NMR spectral signals of **2** were also similar to those of **1**. The only difference was the occurrence of an ethyl group including an oxymethylene at δ_H 3.63 (2H, q, J = 6.9 Hz, H-16)/δ_C 66.5 and a methyl group at δ_H 1.29 (3H, t, J = 6.9 Hz, CH_3-17)/δ_C 15.0. HMBC spectrum of **2** displayed correlations between H-17 (δ 1.29) and C-16 (δ 66.5), and between H-15 (δ 4.66) and C-16 (δ 66.5), suggesting an ethoxy group to be attached at C-15. The ECD spectrum of **2** showed similar pattern with **1**, indicating the same *trans* ring junction and supported the same configurations of 2*S* and 6*R* in **2**.

The ^{1}H and ^{13}C NMR spectra of fomitopin C (**3**) showed similar characteristics with those of **2**, only with the difference of observation of one oxymethine at δ_H 4.70 (1H, m, H-4)/δ_C 71.0. The hydroxyl substitution was evidenced at C-4 according to the ^{1}H–^{1}H COSY correlation between H-4 (δ 4.70) and H-3 (δ 2.43, 1.86), and between H-4 and H-5 (δ 2.22, 2.13). The ECD spectral analysis of **3** revealed similar results to those of **1**, assigned as 2*S* and 6*R*, respectively. Moreover, the absolute configuration at C-4 can be determined as *S via* NOE correlations from H-4 (δ 4.70) to Me-13 (δ 0.87) and therefore, the structure of **3** was established as shown. Comparison of ^{1}H and ^{13}C NMR spectra of fomitopin D (**4**) and **3**, the minor differences were found including the disappearance of an oxymethylene signal and downfield shift of the methyl group [δ_H 3.47 (3H, s, H-16)/δ_C 58.5]. HMBC spectrum of **4** displayed correlation from H-15 (δ 4.62) to C-16 (δ 58.5), revealing a methoxy substitution at C-15 instead of a methyl group in **3**. The ECD and NOESY spectral analysis of **4** determined the same configurations as those of **3** (2*S*, 4*S*, 6*R*).

Table 1 ^{1}H and ^{13}C NMR spectroscopic data of compounds **1–12**

	1[a]		**2**[a]		**3**[b]		**4**[a]		**5**[a]		**6**[a]	
Position	δ_C	δ_H (J in Hz)	δ_C	δ_H (J in Hz)	δ_C	δ_H (J in Hz)	δ_C	δ_H (J in Hz)	δ_C	δ_H (J in Hz)	δ_C	δ_H (J in Hz)
1	173.6		173.6		172.8		172.5		172.4		172.8	
2	50.7		50.7		51.8		51.1		51.1		50.1	
3	29.0	1.76 dd (8.4, 13.9) 2.17 t (13.9)	29.0	1.76 m 2.17 t (11.2)	41.4	1.86 d (13.7) 2.43 dd (8.2, 13.7)	40.5	2.23 dd (7.7, 13.1) 2.34 dd (7.7, 13.4)	40.5	2.24 dd (5.2, 13.1) 2.35 dd (7.9, 13.1)	40.5	1.79 d (14.1) 2.68 dd (8.1, 14.1)
4	19.7	1.97 m	19.7	1.87 m	71.0	4.70 m	71.2	4.73 qd (1.0, 6.0)	71.3	4.75 qd (1.9, 6.7)	71.5	4.78 qd (2.5, 7.7)
5	29.6	1.86 t (8.7) 1.98 m	29.6	1.86 m 1.93 m	41.3	2.13 m 2.22 dd (9.1, 14.0)	40.7	1.90 dd (0.7, 14.4) 2.45 dd (8.4, 14.4)	40.7	1.91 dd (0.8, 13.5) 2.46 dd (9.0, 13.5)	40.9	2.04 dd (5.6, 13.3) 2.44 dd (7.7, 13.3)
6	47.1		47.1		47.2		46.5		46.5		47.6	
7	134.4		134.3		134.3		134.1		134.1		133.7	
8	144.7		144.6		145.5		144.4		144.5		144.5	
9	115.1	6.74 s	115.3	6.71 s	116.4	6.94 s	115.6	6.72 s	115.3	6.74 s	115.3	6.74 s
10	122.9		120.8		124.8		120.6		123.0		123.2	
11	152.9		152.9		152.4		152.9		152.9		153.0	
12	113.0	6.64 s	112.9	6.63 s	112.3	6.62 s	112.6	6.01 s	112.9	6.62 s	112.8	6.63 s
13	19.8	0.93 s	19.8	0.93 s	20.2	0.87 s	20.4	0.90 s	20.4	0.91 s	26.0	1.15 s
14	25.1	1.10 s	25.1	1.11 s	26.6	1.28 s	26.1	1.34 s	26.2	1.35 s	20.6	1.09 s
15	64.4	4.85 s	71.8	4.66 s	68.5	4.53 s	73.7	4.62 s	64.4	4.86 s	64.4	4.86 s
16			66.5	3.63 q (6.9)	66.6	3.57 q (6.4)	58.5	3.47 s				
17			15.0	1.29 t (6.9)	15.5	1.2 t (6.4)						

	7[a]		**8**[b]		**9**[a]		**10**[a]		**11**[a]		**12**[b]	
Position	δ_C	δ_H (J in Hz)	δ_C	δ_H (J in Hz)	δ_C	δ_H (J in Hz)	δ_C	δ_H (J in Hz)	δ_C	δ_H (J in Hz)	δ_C	δ_H (J in Hz)
1	165.8		173.4		172.3		181.8		178.2		25.6	1.20 s
2	54.4		51.7		50.3		53.0		55.7		44.9	
3	206.5		29.8	1.66 dd (5.7, 14.3) 2.08 m	29.0	1.80 m 2.21 m	37.9	1.84 t (8.8) 2.44 td (2.0, 8.8)	37.6	1.61 m 2.47 m	41.5	1.57 m 1.67 m
4	33.9	2.64 m	20.2	1.94 m	19.5	2.00 m	20.9	1.98 m	21.7	1.82 m 1.96 m	20.3	1.75 m
5	25.1	2.16 m 2.28 m	30.4	1.84 t (8.3) 1.95 m	29.5	1.93 m 2.03 m	36.8	1.64 t (9.9) 2.55 td (5.9, 9.9)	38.9	1.81 m 2.44 m	39.7	1.77 m 2.53 t (4.6)
6	43.7		47.3		48.0		55.6		52.6		52.1	
7	131.7		125.2		144.0		157.0		147.5		146.2	
8	143.9		145.4		144.7		116.7	7.05 br s	115.6	6.89 d (2.3)	147.9	
9	115.5	6.78 s	104.6	6.55 s	119.1	7.22 s	160.8		155.5		118.7	6.84 s
10	123.7		144.9		118.8		118.8		125.6		118.3	
11	154.5		142.5		158.9		132.6	7.44 d (8.6)	127.5	7.11 d (7.4)	155.1	
12	112.5	6.74 s	112.2	6.61 s	114.2	6.76 s	119.7	7.07 br d (8.6)	119.3	6.87 dd (2.8, 7.4)	118.5	6.98 s
13	16.3	1.11 s	20.1	0.89 s	19.8	0.96 s	23.0	0.89 s	23.3	0.86 s	27.0	0.78 s
14	25.2	1.23 s	25.7	1.03 s	24.8	1.16 s	26.3	1.38 s	27.0	1.34 s	22.5	1.41 s
15	64.4	4.89 s			195.4	9.83 s	195.8	9.82 s	61.8	4.70 s	195.0	9.75 s

[a] ^{1}H and ^{13}C NMR data (δ) were measured in chloroform-d at 400 and 100 MHz. [b] ^{1}H and ^{13}C NMR data (δ) were measured in acetone-d_6 at 400 and 100 MHz.

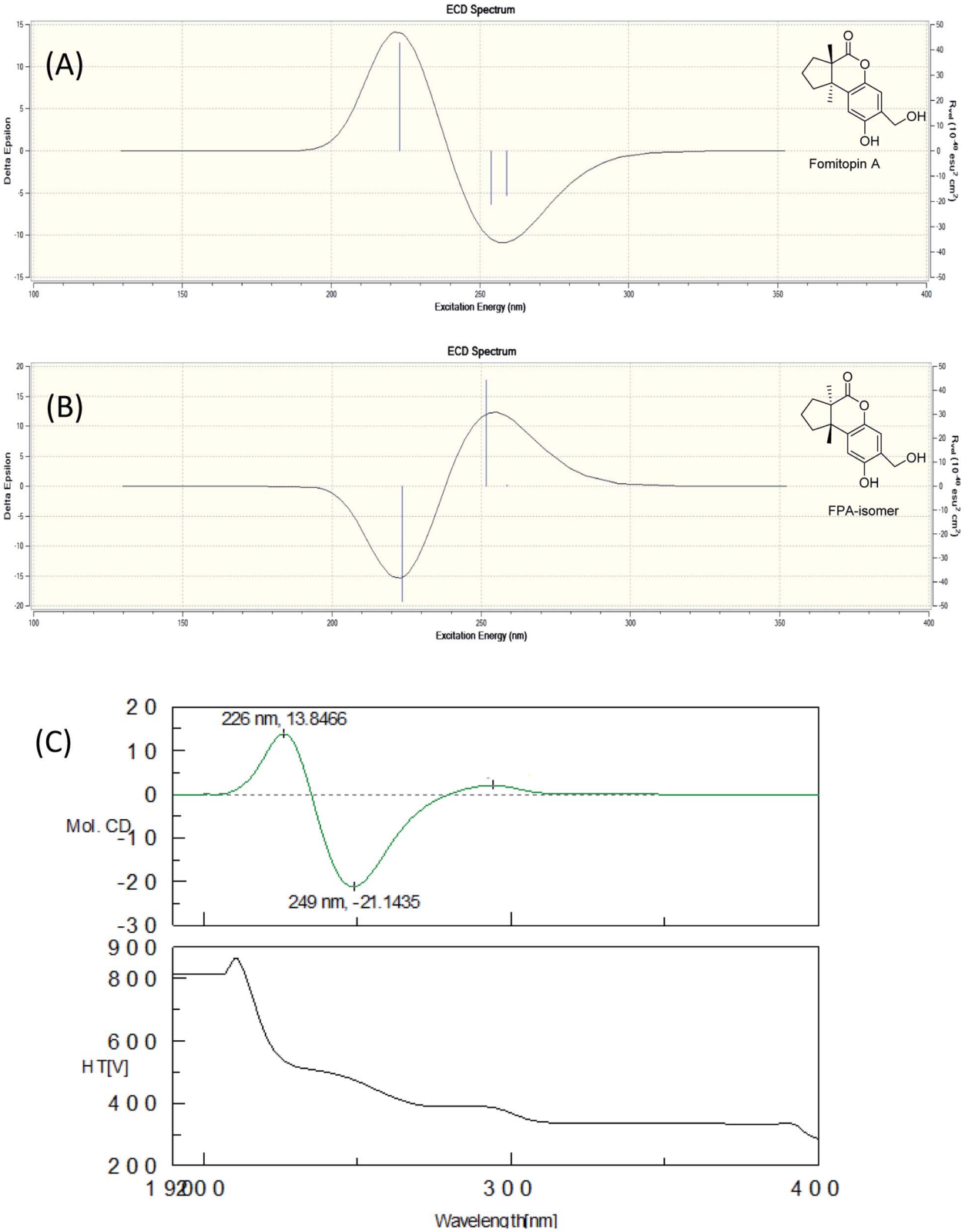

Fig. 1 Simulated ECD spectra of fomitopin A (A) and its isomer (B). Experimental ECD spectrum of fomitopin A (C).

The HRESIMS analytical data of fomitopins E (**5**) and F (**6**) revealed the same molecular formula, and their ^{1}H and ^{13}C NMR spectra were almost identical and very close to those of **4** with the disappearance of a methyl group only, suggesting a free hydroxyl functionality at C-15. The same *trans* ring junction (2*S*, 6*R*) was assigned *via* the ECD spectra of **5** and **6**. Further NOESY

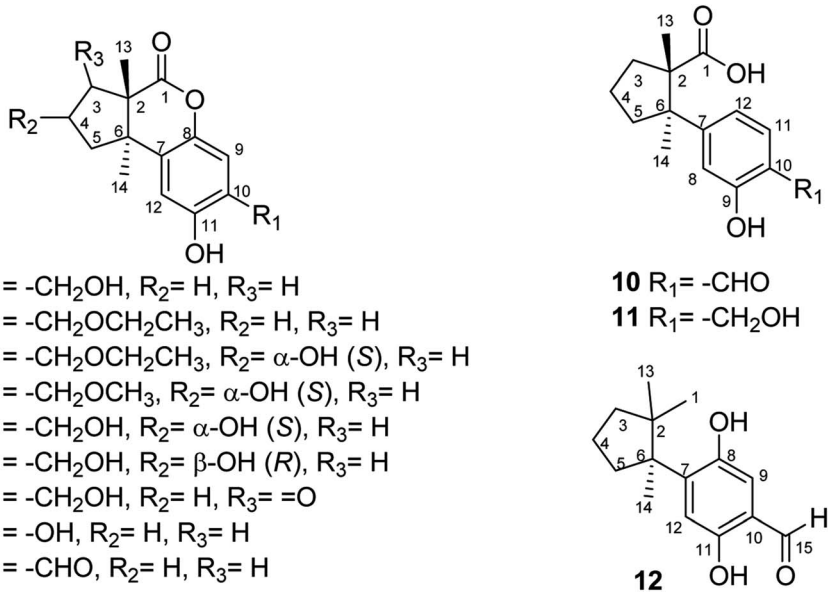

Fig. 2 Structures of fomitopins A–L (**1–12**).

experiments of **6** showed correlations from H-4 (δ 4.79) to Me-14 (δ 1.09), determining OH-4 as β orientation, while OH-4 in **5** is α-orientated supported by correlation from H-4 (δ 4.75) to Me-13 (δ 0.91). Therefore, **5** and **6** were epimers and their structures are shown in Fig. 2. Although compound **2** is only one ethoxy different with **1** and compound **3** and **4** are respectively one methoxy or ethoxy different from compound **5**, we think they are natural products, not artifacts. The reason is that refluxing condition is around 80–90 °C in weakly acidic condition (ethanol). Thus, S_N2 substitution is not favored in acidic condition while S_N1 is not favored in primary carbon. Therefore, these compounds originate from plant materials without doubt.

Comparison of ^1H and ^{13}C NMR spectra of fomitopin G (**7**) with those of **5**, loss of a 4-hydroxy signal but occurrence of a carbonyl carbon at δ 206.5 were observed. HMBC spectrum of **7** showed correlations from both Me-13 (δ 1.11) and Me-14 (δ 1.23) to C-3 (δ 206.5), and ^1H–^1H COSY correlations between H-4 (δ 2.64) and H-5 (δ 2.28, 2.16) can be observed, indicating the

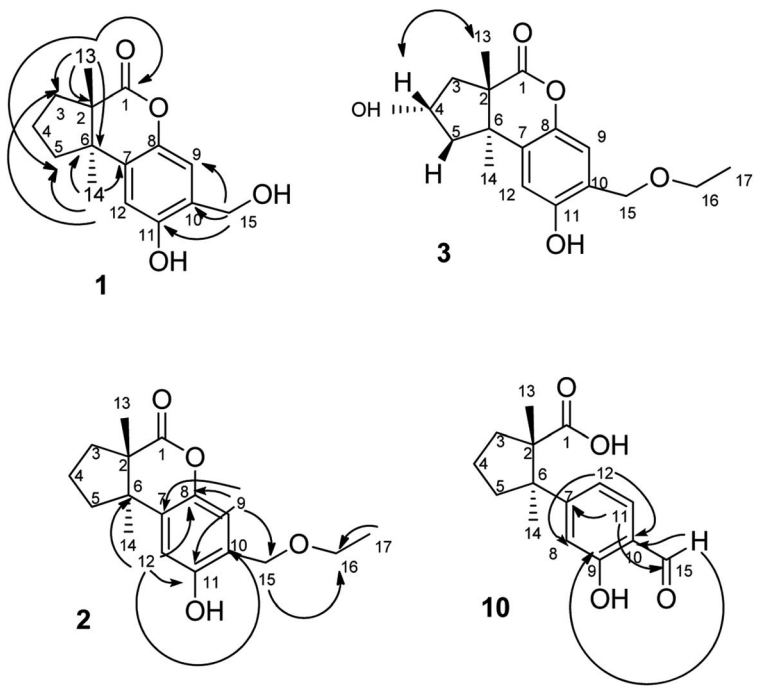

Fig. 3 HMBC (→, $^1H \rightarrow {}^{13}C$) and NOESY (↔, $^1H \rightarrow {}^1H$) correlations of **1**, **2**, **3** and **10**.

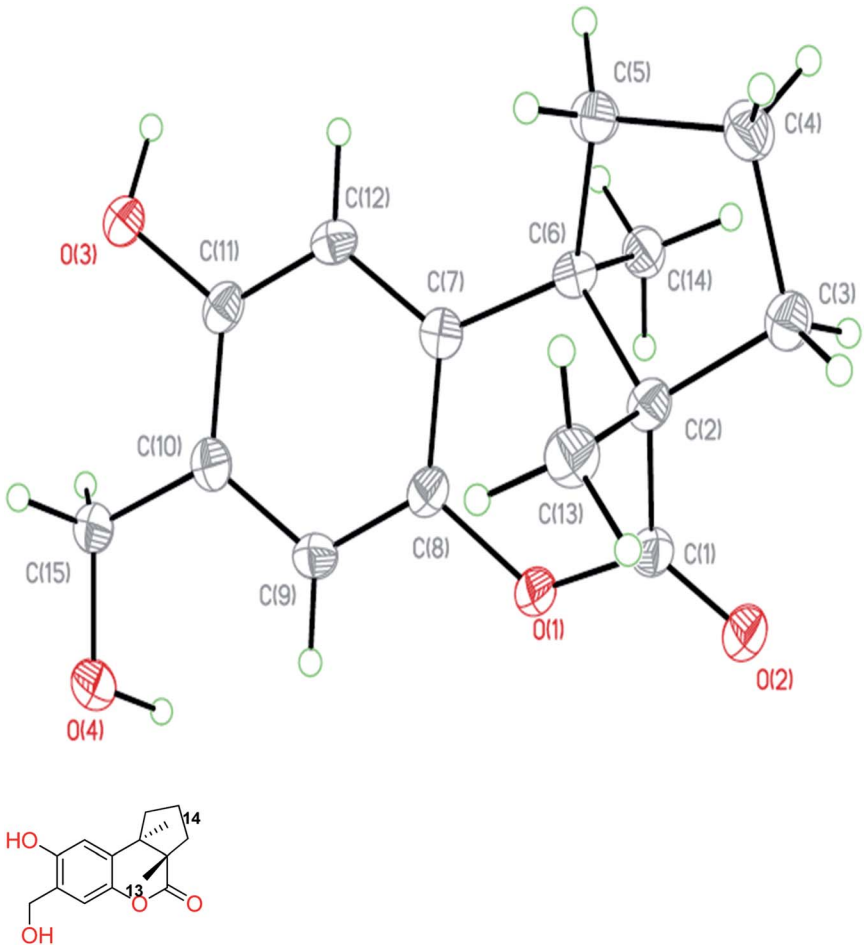

Fig. 4 ORTEP drawing of fomitopin A (**1**).

carbonyl group to be at C-3. The same configurations (2*S*, 6*R*) was assigned *via* ECD spectrum, and fomitopin G (**7**) was established as shown.

The main skeleton of fomitopin H (**8**) was similar to **1**. The minor differences included loss of a methylene signal and downfield shift of a quaternary carbon in both ^{1}H and ^{13}C NMR spectra, which indicated loss of a methylene group and direct substitution of a hydroxyl on aromatic ring. Analysis of HMBC correlations from H-9 (δ 6.74) to C-7 (δ 125.2), C-8 (δ 145.4), C-11 (δ 142.5), and C-10 (δ 144.9); and from H-12 (δ 6.6) to C-6 (δ 47.3), C-8 (δ 145.4), C-10 (δ 144.9) and C-11 (δ 142.5), confirmed C-10 hydroxyl substitution. ECD spectrum of **8** showed similar pattern with **1** that a negative Cotton effect at 253 nm and a positive Cotton effect at 222 nm were found, indicating the same absolute configurations of **8** with **1**. Conclusively, **8** was belonged to an undescribed scaffold norsesquiterpene, and its structure was established as shown.

HRESIMS analysis of fomitopin I (**9**) revealed a molecular formula of $C_{15}H_{16}O_4$. Its IR spectrum showed the typical band for the presence of aromatic aldehyde at 1659 cm^{-1}. The ^{1}H and ^{13}C NMR spectra of **9** were close to those of **8**, with the minor difference of the replacement of phenol group with an aldehyde signal at δ_H 9.83 (1H, s, H-15)/δ_C 195.4. ^{2}J, ^{3}J-HMBC correlations from H-9 (δ 7.22) to C-15 (δ 195.4), and from H-15 (δ 9.83) to C-9 (δ 119.1) and C-11 (δ 158.9), evidenced the aldehyde group to be attached at C-10. The ECD spectrum of **9** showed similar pattern with **1**. According to the above results, the structure of **9** was determined.

The molecular formula of fomitopin J (**10**) was established through HRESIMS analysis. Its IR spectrum displayed the characteristic absorption bands of carboxylic acid (1695 cm^{-1}) and aromatic aldehyde (1654 cm^{-1}). The ^{1}H NMR spectrum of **10** only exhibited minor differences from that of **9**, including the replacement of two aromatic singlets with one ABX set of signals at δ_H 7.44 (1H, d, J = 8.6 Hz, H-11), 7.07 (1H, br d, J = 8.6 Hz, H-12), and 7.05 (1H, br s, H-8). In addition, the change of the lactonic carbon with carboxylic acid functionality (δ_C 178.2) was noticed, suggesting opening of the lactone ring. Further ^{3}J-HMBC correlations from H-8 (δ 7.07) to C-10 (δ 118.8) and C-12 (δ 116.7) supported the substitution pattern of aromatic ring. The *trans* ring junction was proposed *via* NOE correlations from Me-13 (δ 0.89) to H-3β (δ 2.44) and H-5β (δ 2.55), and from Me-14 (δ 1.38) to H-3α (δ 1.84) and H-5α (δ 1.64). The ^{1}H and ^{13}C NMR spectra of fomitopin-K (**11**) were close to those of **1** and the observed differences in **11** were similar to those of **10**, suggesting the ring opening of the lactone group to carboxylic acid

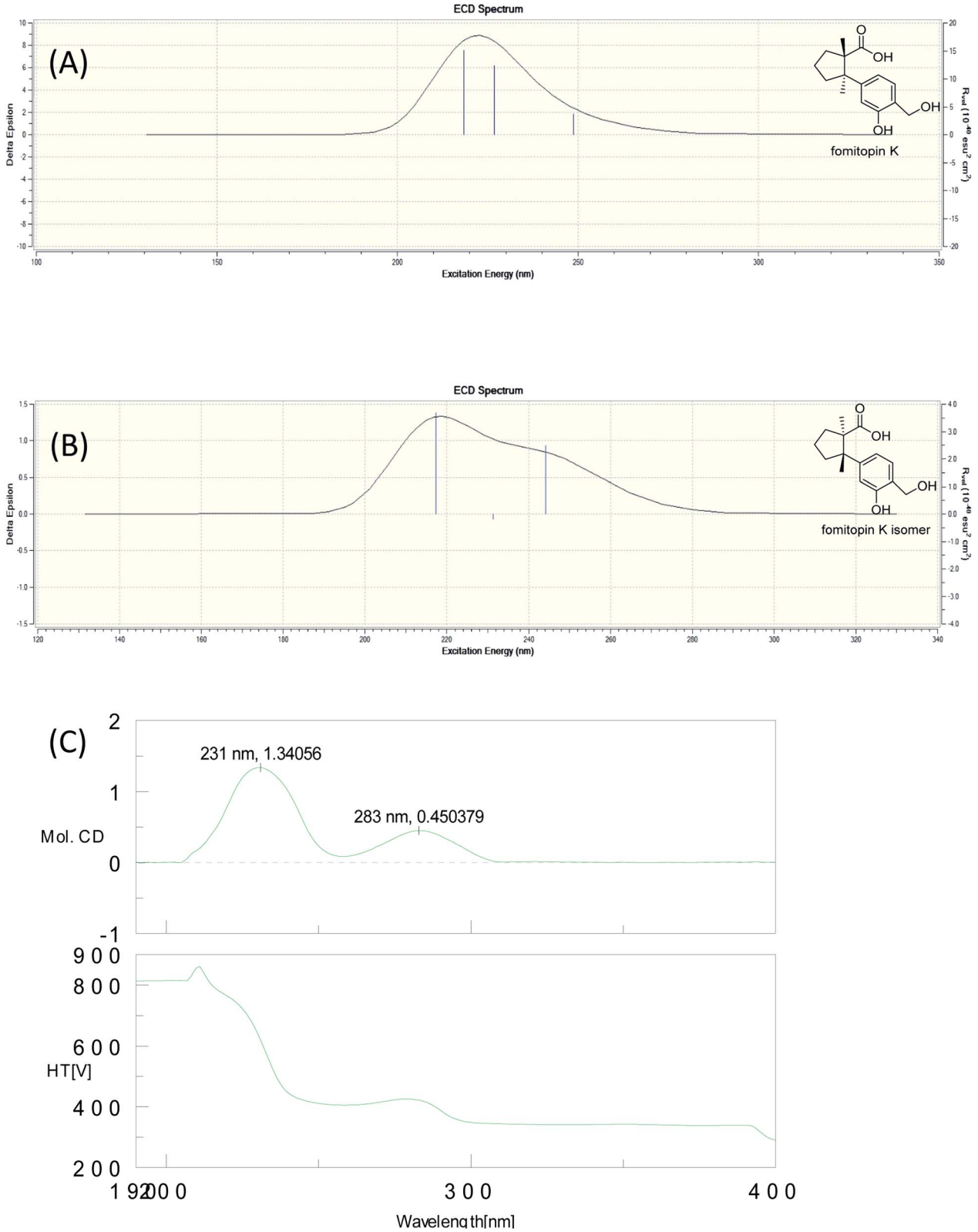

Fig. 5 Simulated ECD spectra of fomitopin K (A) and its isomer (B). Experimental ECD spectrum of fomitopin K (C).

functionality. The IR spectrum of **11** also revealed the presence of carboxylic acid (1693 cm^{-1}). Further HMBC analysis displayed correlations from H-8 (δ 8.89) to C-6 (δ 52.6), C-9 (δ 155.5), C-10 (δ 125.6) and C-12 (δ 119.3), which also supported the speculation. Simulated ECD of **11** revealed the same pattern as the experimental spectrum that two positive Cotton effects

Table 2 Inhibitory effects of isolated compounds on superoxide anion generation and elastase release by human neutrophils in response to fMLP/CB

Compound	IC_{50}[a] (μM)	
	Superoxide anion generation	Elastase release
1	>10	>10
2	>10	>10
4	>10	>10
6	>10	>10
7	>10	>10
8	>10	>10
9	4.02 ± 1.07	6.65 ± 0.68
10	1.66 ± 0.81	4.60 ± 0.26
11	0.81 ± 0.15	0.74 ± 0.12
12	1.72 ± 0.71	3.09 ± 0.45
LY294002[b]	0.4 ± 0.02	1.5 ± 0.3

[a] Concentration necessary for 50% inhibition. The results are presented as the means ± SEM (n = 3–5). [b] A phosphatidylinositol-3-kinase inhibitor was used as a positive control.

were observed around 230 nm and 280 nm, supporting the configurations of 2*S*, 6*R* (Fig. 5). ECD spectrum of **10** revealed the same pattern as those of **11**. Therefore, the structures of **10** and **11** were drawn as shown.

Fomitopin L (**12**) was obtained as colorless solids with a pseudo-molecular formula of $C_{15}H_{20}O_4Na$ determined by HRESIMS ($[M + Na]^+$ peak at m/z 271.1306, calcd for 271.1304), representing six unsaturation equivalents. The UV and IR characteristics of **12** revealed the lack of a carboxylic acid functionality as compared to **10**. The ^1H, ^{13}C, and HSQC NMR spectra revealed two aromatic protons at δ_H 6.84 (1H, s, H-9)/δ_C 118.7 and 6.98 (1H, s, H-12)/δ_C 118.5; one aldehyde at δ_H 9.75 (1H, s, H-15)/δ_C 195.0; three methyls at δ_H 1.20 (3H, s, Me-1)/δ_C 25.6, δ_H 0.78 (3H, s, Me-13)/δ_C 27.0, and δ_H 1.41 (3H, s, Me-14)/δ_C 22.5; four aromatic quaternary carbons at δ 118.3, 146.2, 147.9, 155.1 and two quaternary carbons at δ 44.9, 52.1, respectively. In the HMBC spectrum, ^2J, ^3J-HMBC correlations were observed from Me-1 (δ 1.20) to C-2 (δ 44.9), C-3 (δ 41.5), C-5 (δ 39.7), C-6 (δ 52.1) and C-13 (δ 27.0); from Me-13 (δ 0.78) to C-2 (δ 44.9), C-3 (δ 41.5), C-5 (δ 39.7), and C-6 (δ 52.1); from Me-14 (δ 1.41) to C-2 (δ 44.9), C-3 (δ 41.5), C-5 (δ 39.7), C-6 (δ 52.1), and C-7(δ 144.0). In addition, ^1H–^1H COSY correlations between H-3 (δ 1.67, 1.57) and H-4 (δ 1.75), and between H-4 (δ 1.75) and H-5 (δ 2.53, 1.77) indicated that a 1-methyl-2,2-dimethylcyclopentyl moiety was connected to the aromatic ring. The aromatic substituted pattern was also confirmed by HMBC correlations of H-9 (δ 7.22) to C-7 (δ 146.2), C-8 (δ 147.9), C-11 (δ 155.1), and C-15 (δ 195.0); of H-12 (δ 6.76) to C-6 (δ 52.1), C-8 (δ 147.9), C-10 (δ 118.3), and C-11 (δ 155.1); and of H-15 (δ 9.83) to C-9 (δ 118.7), C-10 (δ 118.3) and C-11 (δ 155.1), respectively. Comparison between the simulated ECD spectra of **12** and its isomer, it indicated the *R* configuration of **12** (Fig. 6). Therefore, the structure of **12** was established as shown.

The anti-inflammatory activities of the isolates were evaluated in a human neutrophil cell model. Ten isolated compounds with enough quantities were submitted for their inhibition on the production of superoxide anion and elastase in human neutrophils with formyl-L-methionyl-L-leucyl-L-phenylalanine/cytochalasin B (fMLP/CB) activation (Table 2).[16] Among the tested compounds, **11** exhibited the most potent anti-inflammatory activity with IC_{50} of 0.81 ± 0.15 μM for inhibition of superoxide anion generation and IC_{50} of 0.74 ± 0.12 μM for inhibition of elastase release. Compound **12** and **10** also exhibited moderate inhibition of superoxide anion generation with IC_{50} of 1.72 ± 0.71 and 1.66 ± 0.81 μM, respectively, compared with the reference compound LY294002 (IC_{50} 0.4 ± 0.02 μM). Among all the compounds, we found the structures with either carboxylic acid (**10**, **11**) or aldehyde (**9**, **12**) would possess good anti-inflammatory activities. Superoxide anion generation and elastase release are markers for inflammations. The different inhibition ability of compounds between these two markers implied the compounds may affect different signal pathways upon the production or release of these two markers. For example, the neutrophil activating agent in this study is fMLP, which can activate fMLP receptor on neutrophil and subsequent p38 mitogen-activated protein kinase (MAPK) signaling pathway to trigger both inflammation markers' production and release.[17] Other mechanisms, such as elevation of intracellular cAMP level, is believed to suppress the activation of neutrophil.[18] Further mechanism studies are needed to address the difference of inhibitory activity. Although the structure of compounds isolated are simple, these kind of sesquiterpenes are rare in the literature and several types of skeletons are discovered in this study. Further, their absolute configuration were solved *via* X-ray crystal structure and simulated ECD and their anti-inflammatory activities were screened, all of which contributes to the progress of natural products development. Moreover, the newly characterized sesquiterpenes can be potential leads for the further anti-inflammatory studies.

Experimental section

General experimental procedures

Melting points were recorded on a Yanaco MP-S3 micro-melting point measuring apparatus without correction. Optical rotations were measured using a JASCO P-2000 digital polarimeter. UV spectra were examined at room temperature on a U-0080-D UV-Vis spectrophotometer. IR spectra were obtained with a PerkinElmer FT-IR Spectrum RX I spectrophotometer. ^1H and ^{13}C NMR spectra were recorded on a Bruker AV III 400 NMR spectrometer. Chemical shifts are shown in δ values (ppm) with tetramethylsilane as an internal standard. The ESIMS and HRESIMS were taken on a Bruker APEX II FT-MS spectrometer (positive-ion mode). ECD spectra were obtained on a JASCO J-720 spectrometer. X-ray single crystal diffraction was measured in National Chung Hsing University with a Bruker D8 VENTURE diffractometer with a Photon 100 CMOS detector system equipped with a Cu Incoatec IμS microfocus source (λ = 1.54178 Å). Column

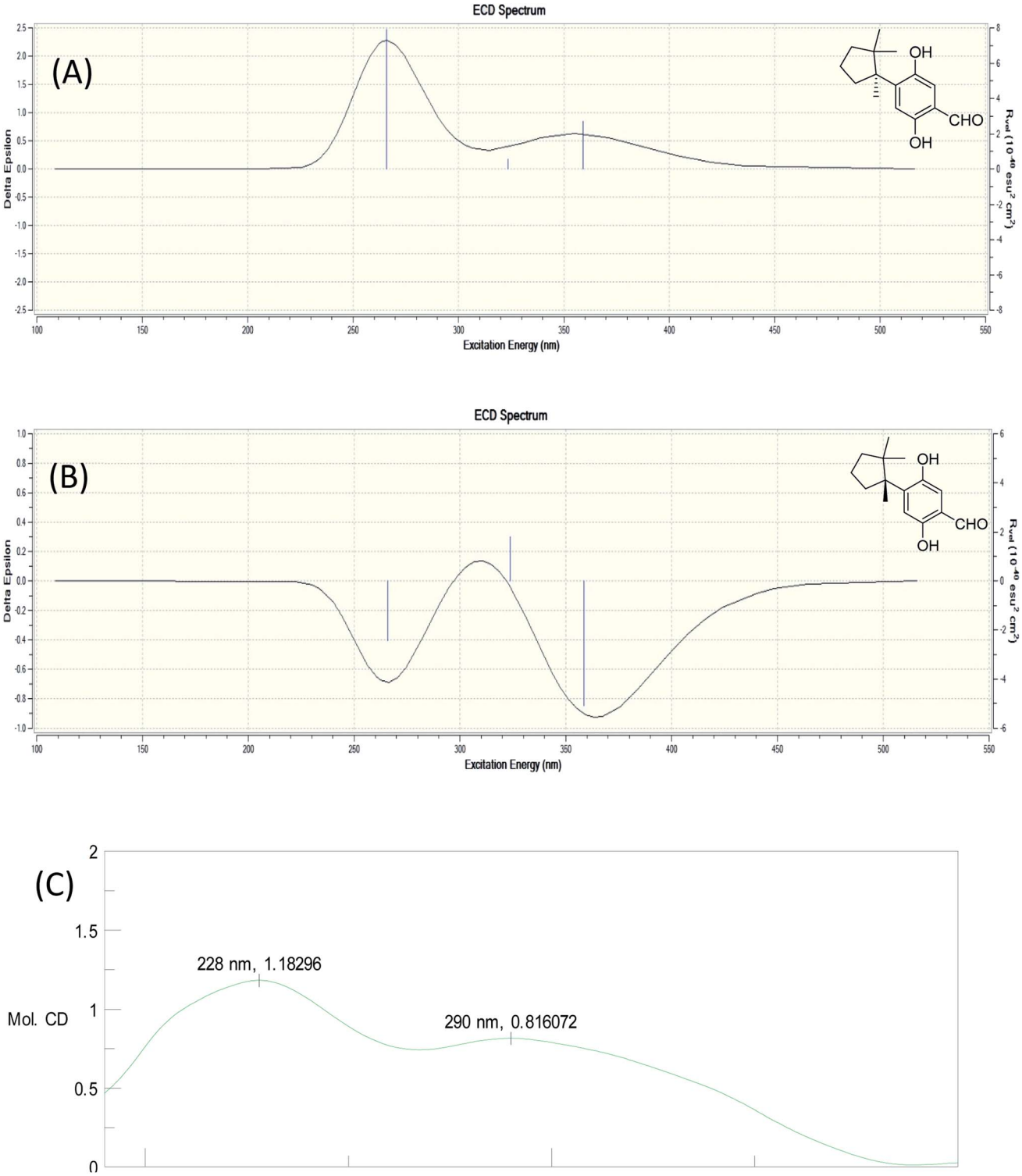

Fig. 6 Simulated ECD spectra of fomitopin L (A) and its isomer (B). Experimental ECD spectrum of fomitopin L (C).

chromatography (CC) was performed on silica (70–230 mesh and 230–400 mesh, Merck) and Diaion HP-20 (Mitsubishi) gels. Preparative thin-layer chromatography (TLC) was conducted on Merck precoated silica gel 60 F254 plates, using UV light to visualize the spots. High-performance liquid chromatography (HPLC) was performed on a Shimadzu LC-20AT series pumping system equipped with a Shimadzu SPD-20A UV-Vis detector, and a SIL-10AF autosampling system at ambient temperature and a RP-18 column (Ascentis C18, 5 μm, 10 mm × 25 cm).

Fungus material

The fruiting bodies of *Fomitopsis pinicola* (Sw.) P. Karst (Fomitopsidaceae) were collected in July 2012 at Qilai Mountain in Hualien, Taiwan. The fungus material was identified by Prof. Jin-Bin Wu, Institute of Pharmaceutical Chemistry and Department of Pharmacy, China Medical University, Taichung, Taiwan. A voucher specimen (TSWu-20130711) was deposited in the School of Pharmacy, National Cheng Kung University, Taiwan.

Extraction and isolation

The fresh fruiting bodies (13.7 kg) were cut into small pieces and consecutively refluxed with ethanol for 8 hours for three times by Jen Li biotech company. The ethanol was removed and evaporated *in vacuo* to yield 3320 g dried extract. The water layer was evaporated *in vacuo* (260 g dried extract). One kilogram of the ethanol extract was subjected to column chromatography on Diaion HP-20 with a step-gradient of water-methanol to give 6 fractions (FP-1–FP-6). And 10 g of ethanol extract was separated at the same condition and was sent to test the bioassay. The bioactive fractions were FP4–FP6. Repeated silica gel column chromatography of the FP-4 fraction (4.64 g) eluted with chloroform–methanol (9 : 1) or isopropyl ether–methanol (7 : 1 or 19 : 1) system yielded four sesquiterpenoids, fomitopin-D (**4**, 26.7 mg), fomitopin-G (**7**, 7.3 mg), fomitopin-E (**5**, 17.11 mg) and fomitopin-F (**6**, 4.39 mg). The FP-5 fraction (15.01 g) eluted with chloroform–acetone (15 : 1) yielded fomitopin-A (**1**, 28.55 mg). Subfraction of FP-5 was chromatographed over silica gel eluted with isopropyl alcohol to give fomitopin-H (**8**, 22.3 mg). Another subfraction of FP-5 eluted with chloroform–methanol (15 : 1) to give fomitopin-K (**11**, 9.8 mg). Fomitopin-C (**3**, 1.2 mg) was obtained from subfraction of FP-5 *via* semipreparative HPLC using RP-18 column and methanol–water (40 : 60) system (retention time: 20.0 min). The last fraction (FP-6, 500 g) eluted with isopropyl ether–acetone yielded 11 subfractions (FP-6-1–P-6-11). FP-6-2 was chromatographed over silica gel with isopropyl ether–acetone (15 : 1) and then isopropyl ether–chloroform–isopropyl alcohol (10 : 19 : 1) system to obtain fomitopin-I (**9**, 2.0 mg) and fomitopin B (**2**, 2.6 mg). Fomitopin-J (**10**, 9.1 mg) was obtained from subfraction of FP-6-10 *via* semipreparative HPLC using RP-18 column and methanol–water (80 : 20 with 0.1% formic acid) system (retention time: 6.0 min). Fomitopin-L (**12**, 1.1 mg) was also obtained from this FP-6-2-5 *via* thin-layer chromatography using chloroform–methanol (15 : 1).

Fomitopin A (1). Colorless needles; mp 176–178 °C; $[\alpha]_D^{25}$ −109.0 (*c* 0.1, MeOH); UV (MeOH) λ_{max} (log ε) 287 (1.7), 242 (2.8), 216 (3.2) nm; ECD (MeOH) (mol. CD) 249 (−21.1), 226 (+13.8) nm; IR (KBr) ν_{max} 3420, 3243, 2972, 1741, 1423, 1377, 1171, 1073, 879, 754 cm^{-1}; ^1H NMR and ^{13}C NMR, see Table 1; HRESIMS *m*/*z* 285.1097 ([M + Na]$^+$ calcd for $C_{15}H_{18}O_4Na$, 285.1097).

Fomitopin B (2). Colorless crystal; $[\alpha]_D^{25}$ −27.2 (*c* 0.1, MeOH); UV (MeOH) λ_{max} (log ε): 287 (1.2), 241 (2.3), 216 (3.0) nm; ECD (MeOH) (Mol. CD) 249 (−4.9), 224 (2.6) nm; IR (KBr) ν_{max} 3373, 2967, 2879, 1768, 1741, 1587, 1425, 1175, 1098, 755 cm^{-1}; ^1H NMR and ^{13}C NMR: see Table 1; HRESIMS *m*/*z* 313.1407 ([M + Na]$^+$ calcd 313.1410).

Fomitopin C (3). Colorless solid; $[\alpha]_D^{25}$ −35.4 (*c* 0.1, MeOH); UV (MeOH) λ_{max} (log ε): 287 (1.2), 241 (1.9), 217 (3.0) nm; ECD (MeOH) (mol. CD) 253 (−6.1), 222 (3.7) nm; IR (KBr) ν_{max} 3362, 2928, 1760, 1587, 1427, 1381, 1267, 1178, 1015, 755 cm^{-1}; ^1H NMR and ^{13}C NMR: see Table 1; HRESIMS *m*/*z* 329.1358 ([M + Na]$^+$ calcd 329.1359).

Fomitopin D (4). Colorless needles; $[\alpha]_D^{25}$ −72.2 (*c* 0.1, MeOH); UV (MeOH) λ_{max} (log ε): 287 (1.1), 242 (1.7), 214 (2.6) nm; ECD (MeOH) (mol. CD) 251 (−9.9), 222 (5.6) nm; IR (KBr) ν_{max} 3309, 2964, 2829, 1766, 1759, 1748, 1627, 1496, 1427, 1264, 1174, 1080, 755 cm^{-1}. ^1H NMR and ^{13}C NMR: see Table 1; HRESIMS *m*/*z* 315.1200 ([M + Na]$^+$ calcd 315.1202).

Fomitopin E (5). Colorless needles; $[\alpha]_D^{25}$ −86.3 (*c* 0.6, MeOH); UV (MeOH) λ_{max} (log ε) 287 (1.6), 243 (2.7), 215 (3.3) nm; ECD (MeOH) (Mol. CD) 251 (−10.0), 222 (4.6) nm; IR (KBr) ν_{max} 3708, 2969, 2873, 1755, 1427, 1278, 1173, 1075, 1014, 754 cm^{-1}; ^1H NMR and ^{13}C NMR: see Table 1; HRESIMS *m*/*z* 301.1045 ([M + Na]$^+$ calcd 301.1046).

Fomitopin F (6). Colorless needles; $[\alpha]_D^{25}$ −52.9 (*c* 0.1, MeOH); UV (MeOH) λ_{max} (log ε) 287 (1.0), 242 (1.8), 212 (3.3) nm; ECD (MeOH) (mol. CD) 251 (−8.0), 222 (3.9) nm; IR (KBr) ν_{max} 3706, 2957, 2845, 1755, 1427, 1280, 1174, 1084, 1014, 755 cm^{-1}; ^1H NMR and ^{13}C NMR: see Table 1; HRESIMS *m*/*z* 301.1045 ([M + Na]$^+$ calcd 301.1046).

Fomitopin G (7). Colorless needles; $[\alpha]_D^{25}$ −37.4 (*c* 0.2, MeOH); UV (MeOH) λ_{max} (log ε) 286 (1.2), 237 (2.7), 215 (3.3) nm; ECD (MeOH) (mol. CD) 252 (−3.3), 222 (1.4) nm; IR (KBr) ν_{max} 3381, 2930, 2877, 1778, 1747, 1427, 1282, 1174, 1080, 756 cm^{-1}.^1H NMR and ^{13}C NMR: see Table 1; HRESIMS *m*/*z* 299.0887 ([M + Na]$^+$ calcd 299.0889).

Fomitopin H (8). Colorless crystal; $[\alpha]_D^{25}$ −94.4 (*c* 0.1, MeOH); UV (MeOH) λ_{max} (log ε) 291 (1.6), 248 (1.2), 214 (3.6) nm; ECD (MeOH) (mol. CD) 253 (−6.8), 222 (2.9) nm; IR (KBr) ν_{max} 3386, 2967, 2931, 1746, 1628, 1509, 1444, 1138, 1099, 756 cm^{-1}; ^1H NMR and ^{13}C NMR: see Table 1; HRESIMS *m*/*z* 271.0938 ([M + Na]$^+$ calcd 271.0940).

Fomitopin I (9). Colorless solid; $[\alpha]_D^{25}$ −22.7 (*c* 0.1, MeOH); UV (MeOH) λ_{max} (log ε) 339, 258, 231 nm; ECD (MeOH) (mMol. CD) 240 (−6.8), 216 (2.5) nm; IR (KBr) ν_{max} 2962, 2930, 1775, 1659, 1576, 1432, 1378, 1223, 1142, 1068, 883 cm^{-1}; ^1H NMR and ^{13}C NMR: see Table 1; HRESIMS *m*/*z* 283.0940 ([M + Na]$^+$ calcd 283.0940).

Fomitopin J (10). Colorless solid; $[\alpha]_D^{25}$ +8.2 (*c* 0.1, MeOH); UV (MeOH) λ_{max} (log ε) 329 (1.4), 263 (3.5), 217 (3.3) nm; ECD (MeOH) (mol. CD) 270 (1.3) nm; IR (KBr) ν_{max} 3684, 2963, 2879, 1695, 1654, 1561, 1506, 1458, 1064, 757 cm^{-1}; ^1H NMR and ^{13}C NMR: see Table 1; HRESIMS *m*/*z* 285.1098 ([M + Na]$^+$ calcd 285.1097).

Fomitopin K (11). Colorless needles; $[\alpha]_D^{25}$ +10.5 (*c* 0.3, MeOH); UV (MeOH) λ_{max} (log ε) 276 (2.2), 230 (3.4), 218 (2.4) nm; ECD (MeOH) (mol. CD) 283 (0.5), 231 (1.3) nm; IR (KBr) ν_{max} 3328, 2970, 1693, 1623, 1579, 1509, 1417, 1379, 1209, 757 cm^{-1}; ^1H NMR and ^{13}C NMR: see Table 1; HRESIMS *m*/*z* 287.1255 ([M + Na]$^+$ calcd 287.1253).

Fomitopin L (12). Colorless solid; $[\alpha]_D^{25}$ −43.9 (*c* 0.1, MeOH); UV (MeOH) λ_{max} (log ε) 270 (0.6), 219 (3.6) nm; ECD (MeOH) (mol. CD) 290 (0.8), 228 (1.2) nm; IR (KBr) ν_{max} 3472, 2955, 2929, 2879, 1666, 1617, 1440, 1410, 1246, 1132 cm^{-1}; ^1H NMR and ^{13}C NMR: see Table 1; HRESIMS *m*/*z* 271.1306 ([M + Na]$^+$ calcd 271.1304).

Single-crystal X-ray diffraction analysis and crystallographic data for compound 1

The diffraction intensity data for compound **1** were acquired on a Bruker D8 Venture with a Photon 100 CMOS detector system equipped with a Cu INCOATEC IμS microfocus source (λ = 1.54178 Å). The data were collected by Bruker APEX2 software. The data reductions were conducted with Bruker SAINT. Structure solutions and refinements were performed with the SHELXTL program package. The crystal structures of compound **1** was drawn by ORTEP (Fig. 4).

Crystallographic data of 1

$C_{15}H_{18}O_4$, formula weight 262.29, space group $P2_12_12_1$, a = 6.6564(2) Å, b = 10.3704(3) Å, c = 17.9622(6) Å, $\alpha = \beta = \gamma = 90°$, V = 1239.92(7) Å^3, Z = 4, D_{calcd} = 1.405 mg m^{-3}, crystal dimensions 0.45 × 0.36 × 0.32 mm^3 were used for measurements on a Bruker D8 VENTURE diffractometer with a graphite monochromator (Φ/ω scans, $2\theta_{max}$ = 72.19°), Cu Kα radiation. The total number of independent reflections measured was 2382, of which 4664 were observed. Final indices: R_1 = 0.0375, wR_2 = 0.0975, S = 1.022.

The crystallographic data for the structures of fomitopin A has been deposited with the Cambridge Crystallographic Data Centre (deposit numbers CCDC 1573301).

ECD spectrum calculation. The TDDFT ECD spectra were calculated at the B3LYP/6-31G(d,p)//B3LYP/6-31G(d,p) level of theory using Gaussian 09.[19] Results were visualized in GaussView 5.0. Calculations were performed with the conductor-like screening model (COSMO) to account for the electrostatic interaction of the molecule with methanol as solvent.[21]

Human neutrophil preparation. A standard method of dextran sedimentation was performed to isolate neutrophils prior to centrifugation in a Ficoll Hypaque gradient and hypotonic lysis of erythrocytes. Healthy donors' (20–30 years old) whole blood was drawn by venipuncture with a protocol approved by Chang Gung Memorial Hospital (IRB protocol number: 102-1595A3) review board.[20] Before use, the purified neutrophils were maintained at 4 °C in a Ca^{2+}-free Hank's balanced salt solution (HBSS) buffer at pH 7.4.

All experiments were performed in accordance with the Guidelines of the Institutional Review Board at Chang Gung Memorial Hospital, and experiments were approved by the ethics committee at Chang Gung Memorial Hospital. Informed consents were obtained from human participants of this study.

Superoxide anion generation measurement. Using the principle of the reduction of ferricytochrome *c* can be inhibited by superoxide dismutase (SOD) leaded to develop a superoxide anion generation assay.[20] Each test compound or an equal volume of vehicle (0.1% DMSO, negative control) was incubated for 5 min with neutrophils (6 × 10^5 cells per mL) equilibrated with 0.5 mg mL^{-1} ferricytochrome *c* and 1 mM Ca^{2+} at 37 °C for 2 min. Cells were first incubated with cytochalasin B (CB, 1 μg mL^{-1}) for 3 min, and then activated by formyl-L-methionyl-L-leucyl-L-phenylalanine (FMLP, 100 nM). The changes in absorbance with reduction of ferricytochrome *c* at 550 nm were continuously monitored in a double-beam, six-cell positioned spectrophotometer (Hitachi U-3010, Tokyo, Japan) with constant stirring. Calculations were done from differences in the reduction with and without SOD (100 U per mL) divided by the extinction coefficient for the reduction of ferricytochrome *c* (ε = 21.1/mM/10 mm). LY294002 [2-(4-morpholinyl)-8-phenyl-1(4*H*)-benzopyran-4-one] was used as a positive control.

Elastase release assay. Degranulation of azurophilic granules was determined by elastase release as described previously.[20] MeO-Suc-Ala-Ala-Pro-Val-*p*-nitroanilide was used as the elastase substrate. Neutrophils (6 × 10^5 cells per mL) equilibrated in MeO-Suc-Ala-Ala-Pro-Val-*p*-nitroanilide (100 μM), at 37 °C for 2 min were then incubated with test compounds or an equal volume of vehicle (0.1% DMSO, negative control) for 5 min. Cells were activated by 100 nM FMLP and 0.5 μg mL^{-1} CB, and changes in absorbance at 405 nm were monitored continuously to measure elastase release. The results were expressed as the percentage of elastase release in the FMLP/CB-activated, drug-free control system. LY294002 was used as a positive control.

Statistical analysis. Results were expressed as mean ± SD. Calculations of 50% inhibitory concentrations (IC_{50}) were computer-assisted (PHARM/PCS v.4.2). Statistical comparisons were made between groups using the Student's *t* test. Values of *p* less than 0.05 were considered to be statistically significant.

Conflicts of interest

The authors declare no competing financial interest.

Acknowledgements

This study is sponsored by the Ministry of Science and Technology, Taiwan. Authors are also thankful to Chang Gung Memorial Hospital (CMRPD1B0281–3, CMRPF1D0442–3, CMRPF 1F0011–3, CMRPF1F0061–3 and BMRP450 granted to T.-L. H.) for the partial financial support for the present research.

References

1 G. Bhattarai, Y. H. Lee, N. H. Lee, I. K. Lee, B. S. Yun, P. H. Hwang and H. K. Yi, *Biol. Pharm. Bull.*, 2012, **35**, 1711–1719.
2 M. Popova, B. Trusheva, M. Gyosheva, I. Tsvetkova and V. Bankova, *Fitoterapia*, 2009, **80**, 263–266.
3 C. H. Hwang, B. U. Jaki, L. L. Klein, D. C. Lankin, J. B. McAlpine, J. G. Napolitano, N. A. Fryling, S. G. Franzblau, S. H. Cho, P. E. Stamets, Y. Wang and G. F. Pauli, *J. Nat. Prod.*, 2013, **76**, 1916–1922.
4 J.-E. Haight, G. A. Laursen, J. A. Glaeser and D. L. Taylor, *Mycologia*, 2016, **108**, 925–938.

5 U. Grienke, M. Zöll, U. Peintner and J. M. Rollinger, *J. Ethnopharmacol.*, 2014, **154**, 564–583.
6 D. Choi, S.-S. Park, J.-L. Ding and W.-S. Cha, *Biotechnol. Bioprocess Eng.*, 2007, **12**, 516.
7 S. I. Lee, J. S. Kim, S. H. Oh, K. Y. Park, H. G. Lee and S. D. Kim, *J. Med. Food*, 2008, **11**, 518–524.
8 W.-S. Cha, J.-L. Ding, H.-J. Shin, J.-S. Kim, Y.-S. Kim, D. Choi, H.-D. Lee, H.-B. Kang and C.-W. Lee, *Korean J. Chem. Eng.*, 2009, **26**, 1696–1699.
9 A. C. Keller, M. P. Maillard and K. Hostettmann, *Phytochemistry*, 1996, **41**, 1041–1046.
10 M. T. Heneka, M. J. Carson, J. E. Khoury, G. E. Landreth, F. Brosseron, D. L. Feinstein, A. H. Jacobs, T. Wyss-Coray, J. Vitorica, R. M. Ransohoff, K. Herrup, S. A. Frautschy, B. Finsen, G. C. Brown, A. Verkhratsky, K. Yamanaka, J. Koistinaho, E. Latz, A. Halle, G. C. Petzold, T. Town, D. Morgan, M. L. Shinohara, V. H. Perry, C. Holmes, N. G. Bazan, D. J. Brooks, S. Hunot, B. Joseph, N. Deigendesch, O. Garaschuk, E. Boddeke, C. A. Dinarello, J. C. Breitner, G. M. Cole, D. T. Golenbock and M. P. Kummer, *Lancet Neurol.*, 2015, **14**, 388–405.
11 K. Yoshikawa, M. Inoue, Y. Matsumoto, C. Sakakibara, H. Miyataka, H. Matsumoto and S. Arihara, *J. Nat. Prod.*, 2005, **68**, 69–73.
12 J.-J. Cheng, C.-Y. Lin, H.-S. Lur, H.-P. Chen and M.-K. Lu, *Process Biochem.*, 2008, **43**, 829–834.
13 K. M. Pietrosimone and P. Liu, *World J. Transl. Med.*, 2015, **4**, 60–68.
14 A. Matsuo, S. Yuki and M. Nakayama, *J. Chem. Soc., Perkin Trans. 1*, 1986, 701–710.
15 T. Eicher, F. Servet and A. Speicher, *Synthesis*, 1996, 863–870.
16 P. C. Kuo, H. Y. Hung, C. W. Nian, T. L. Hwang, J. C. Cheng, D. H. Kuo, E. J. Lee, S. H. Tai and T. S. Wu, *J. Nat. Prod.*, 2017, **80**, 1055–1064.
17 D. A. Partrick, E. E. Moore, P. J. Offner, D. R. Meldrum, D. Y. Tamura, J. L. Johnson and C. C. Silliman, *Arch. Surg.*, 2000, **135**, 219–225.
18 T. L. Hwang, S. H. Yeh, Y. L. Leu, C. Y. Chern and H. C. Hsu, *Br. J. Pharmacol.*, 2006, **148**, 78–87.
19 A. E. Nugroho and H. Morita, *J. Nat. Med.*, 2014, **68**, 1–10.
20 S.-C. Yang, P.-J. Chung, C.-Y. Kuo, M.-F. Hung, Y.-T. Huang, W.-Y. Chang, Y.-W. Chang, K.-H. Chan and T.-L. Hwang, *J. Immunol.*, 2013, **190**, 6511–6519.
21 M. J. Frisch, G. W. Trucks, H. B. Schlegel, G. E. Scuseria, M. A. Robb, J. R. Cheeseman, G. Scalmani, V. Barone, B. Mennucci, G. A. Petersson, H. Nakatsuji, M. Caricato, X. Li, H. P. Hratchian, A. F. Izmaylov, J. Bloino, G. Zheng, J. L. Sonnenberg, M. Hada, M. Ehara, K. Toyota, R. Fukuda, J. Hasegawa, M. Ishida, T. Nakajima, Y. Honda, O. Kitao, H. Nakai, T. Vreven, J. A. Montgomery Jr., J. E. Peralta, F. Ogliaro, M. Bearpark, J. J. Heyd, E. Brothers, K. N. Kudin, V. N. Staroverov, T. Keith, R. Kobayashi, J. Normand, K. Raghavachari, A. Rendell, J. C. Burant, S. S. Iyengar, J. Tomasi, M. Cossi, N. Rega, J. M. Millam, M. Klene, J. E. Knox, J. B. Cross, V. Bakken, C. Adamo, J. Jaramillo, R. Gomperts, R. E. Stratmann, O. Yazyev, A. J. Austin, R. Cammi, C. Pomelli, J. W. Ochterski, R. L. Martin, K. Morokuma, V. G. Zakrzewski, G. A. Voth, P. Salvador, J. J. Dannenberg, S. Dapprich, A. D. Daniels, O. Farkas, J. B. Foresman, J. V. Ortiz, J. Cioslowski, and D. J. Fox, *Gaussian 09, Revision E.01*, Gaussian, Inc., Wallingford CT, 2013.